Available online at www.sciencedirect.com

SciVerse ScienceDirect

Procedia Engineering 36 (2012) 516 – 520

Procedia Engineering

www.elsevier.com/locate/procedia

IUMRS-ICA 2011

Magnetic Properties of Oxygen-doping Fe-Co-based Nanocrystalline Alloy Films for High Frequency Application

Hao Geng[a], Yuan Wang[a], Shuangjun Nie[a], Laisen Wang[a], Yuanzhi Chen[a], and Dong-Liang Peng[a,*]

[a]*Department of Materials Science and Engineering, College of Materials, Xiamen University, Xiamen 361005, P. R. China*

Abstract

The effects of the introduction of oxygen were studied on the $Fe_{62}Co_{32}Cr_6$–O alloy films synthesized by magnetron co-sputtering. The as-deposited films exhibited a high saturation magnetization and a suitable in-plane uniaxial anisotropy field at an optimized condition of an oxygen gas flow ratio of 1.3%. Also, a high real permeability of ~200 at frequency up to 3.3 GHz was obtained from the microwave permeability measurement at the optimized condition above. The combination of high saturation magnetization, adjustable in-plane uniaxial magnetic anisotropy field, and high resistivity makes the $Fe_{62}Co_{32}Cr_6$–O films become a promising candidate for the high-frequency applications.

Keywords: Magnetic anisotropy; high-frequency characteristics; oxygen-doping; magnetic materials; sputtering

1. Introduction

Recent improvements in radio frequency integrated circuits (RFICs) have led to a demand for further miniaturization, integration and higher frequency operation in gigahertz (GHz) range of magnetic devices. The basic requirements for the soft magnetic film materials operated in the GHz range include high saturation magnetization (M_s), lower coercivity (H_c), high permeability (μ'), appropriate large anisotropy field (H_k) (to obtain high ferromagnetic resonance frequency (f_r)), and high resistivity (ρ) (to effectively suppress eddy current loss). Although the traditional ferrite films have high resistivity, they are inapplicable in the GHz range RF magnetic devices as a result of their low M_s and the high-temperature

* Corresponding author. Tel.: +86-592-2180155; fax: +86-592-2183515.
E-mail address: dlpeng@xmu.edu.cn.

1877-7058 © 2012 Published by Elsevier Ltd. Open access under CC BY-NC-ND license.
doi:10.1016/j.proeng.2012.03.075

preparation processing. Due to the advantages of high M_s and high μ, Fe-Co based soft magnetic films oriented to microwave applications have received interest in recent years, such as planar inductors and film transformers in integrated circuits [1-2]. Up to now, a great deal of research effort has been devoted to exploring some Fe-Co based films with excellent soft-magnetic properties and high frequency (GHz range) characteristics by altering the film composition and structure. For example, the nanocrystalline or granular Fe-Co(Fe, Co)–X–(oxide, nitride and fluoride) thin film system, with X = Al, Zn, Zr, Si, rare earth, etc., has been investigated as a subject of the candidates for high-frequency applications [3-7]. However, large M_s cannot be achieved because of the addition of nonmagnetic insulants in these systems. In search of a film material with high saturation magnetization and other comprehensive performances, some researchers doped Fe-Co with Cr in the range of 0 – 13 at. % to obtain FeCoCr films [8], while the system's resistivity is still too low to suppress the eddy current loss efficiently in the GHz range. In some previous literatures, the addition of very low dose of oxygen could improve the resistivity and adjust the in-plane uniaxial magnetic anisotropy (IPUMA) in the Fe-Co based nanocrystalline alloy film effectively [9]. Therefore, in this paper, we investigate the effects of oxygen concentration on the microstructural and magnetic properties of Cr-doped Fe-Co based nanocrystalline alloy films, and expect to obtain good high-frequency magnetic characteristics in the GHz range.

2. Experimental

Nanocrystalline $Fe_{62}Co_{32}Cr_6$–O magnetic thin films were prepared on glass slides and (100)-oriented silicon substrates with a thickness of 0.5 mm by magnetron co-sputtering at room temperature. The sputtering chamber was evacuated to a background pressure below 4×10^{-4} Pa. During the sputtering, the Ar gas flow rate and the total gas pressure were maintained at 20 sccm (sccm denotes standard-state cubic centimeter per minute) and 0.4 Pa, respectively. To obtain $Fe_{62}Co_{32}Cr_6$–O alloy films with different oxygen contents, the relative O_2 flow ratio, $R(O_2)$ = [O_2 flow rate]/ [Ar flow rate + O_2 flow rate] (in %), was tuned in the range of 0 to 6.3%. All the depositions were conducted at a $Fe_{65}Co_{35}$ (at. %) alloy target power of 100 W and a pure Cr target power of 80 W. The chemical compositions of the nanocrystalline alloy films were determined by electron probe microanalyzer (EPMA, JEOL-8100). The static magnetic properties of the $Fe_{62}Co_{32}Cr_6$–O films were characterized by using a vibrating sample magnetometer (TOEI VSM-5-15), and then H_k was determined by calculating the measured easy-axis and hard-axis loops of the reduced magnetization. After deposition, the film thicknesses, t, were measured by using a surface profiler (Dektak 3). In this study, the thicknesses of all films were well controlled at about 120 nm by adjusting the sputtering time. Samples were characterized structurally by X-ray diffraction (Panalytical X'pert-PRO) with Cu Kα radiation. For morphological observation, a scanning electron microscope (LEO-1530FE) was used. The microwave permeability measurements of the samples were obtained from 500 MHz to 5 GHz with a vector network analyzer by a shorted microstrip transmission-line perturbation method [10].

3. Results and Discussion

3.1. Structural and morphological characterization

Figure 1 shows the X-ray diffraction patterns of $Fe_{62}Co_{32}Cr_6$–O alloy films prepared at different oxygen flow ratio. The patterns only exhibit diffraction peaks from the (110) and (200) planes of bcc phase $Fe_{62}Co_{32}Cr_6$ alloys and no diffraction peaks for $Fe_{62}Co_{32}Cr_6$ oxide phases were detected in the XRD patterns as $R(O_2)$ increased up to 2.6%. The width of the diffraction peaks becomes wider and the peak height decreases drastically but the position of the peak does not change with increasing oxygen flow

ratio from $R(O_2) = 0$ to 2.6%, which implies that the introduction of oxygen reduced the grain size and the grain surfaces were lightly oxidized. When $R(O_2)$ increases to 6.2%, the diffraction peaks which are referred to $Fe_{62}Co_{32}Cr_6$ alloys phase are vanished but still no diffraction peaks for oxide phases were detected. This indicates that the addition of high dose of oxygen severely distorts the Fe-Co-Cr lattice, so that the film may consist of infinitesimal crystallites or has an amorphous structure.

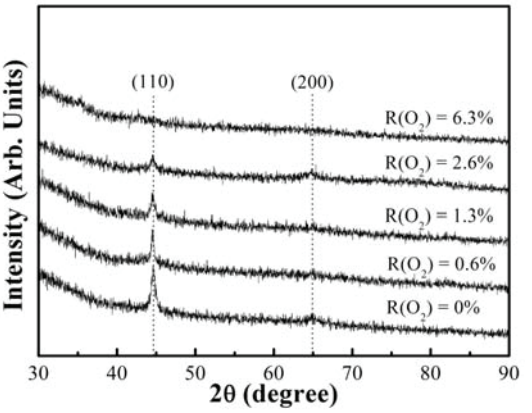

Fig. 1. XRD patterns of $Fe_{62}Co_{32}Cr_6$–O thin films prepared at different $R(O_2)$.

To further investigate the effects of oxygen concentration on the microstructure of $Fe_{62}Co_{32}Cr_6$–O alloy films, we observed the surface morphology using scanning electron microscopy (SEM). As can be seen from Fig. 2, the surface of the films becomes smooth and the grain size gradually decreases with increasing the oxygen gas flow ratio. This result is consistent with the XRD results.

3.2. Magnetism and high-frequency characteristics analysis

Figure 3 shows the in-plane hysteresis loops of $Fe_{62}Co_{32}Cr_6$–O films prepared with various $R(O_2)$. As shown in Fig. 3, the films show an evident IPUMA as $R(O_2)$ increases up to 1.3%. Here the easy axis is along the tangential direction of the wafer rotation, while the hard axis along the radial direction. Such an evident IPUMA can mainly be attributed to the preferential orientation of $Fe_{62}Co_{32}Cr_6$–O crystallite growth, which originates from slantwise atom incidence due to the substrate rotation. Moreover, the IPUMA of the $Fe_{62}Co_{32}Cr_6$–O thin films can be adjusted by introducing low-dose oxygen into the films. It is worth emphasizing that we did not apply an inducing magnetic field during deposition. Besides, from the Fig. 3, the pure $Fe_{62}Co_{32}Cr_6$ alloy thin film without oxygen adding ($R(O_2) = 0$) does not reveal obvious magnetic anisotropy. At the same time, slantwise atom incidence caused by the substrate rotation could give rise to the crystallite growth in the preferential orientation. Therefore, the combination of the refinement of grain size, the light surface oxidization, and the preferential orientation of $Fe_{62}Co_{32}Cr_6$ grains can possibly play an important role in the IPUMA characteristics of the $Fe_{62}Co_{32}Cr_6$–O films. With increasing $R(O_2)$ from 0 to 1.3%, the anisotropy field H_k raises to 43 Oe markedly, while the coercivity of the easy axis and hard axis monotonically decreases, which is consistent with grain refinement as mentioned above. However, the saturation magnetization M_s decreases inevitably from 22.6 to 19.4 kG with increasing $R(O_2)$ from 0 to 1.3%.

As mentioned above, the $Fe_{62}Co_{32}Cr_6$–O films with high saturation magnetization M_s and larger and adjustable IPUMA field H_k can be obtained by the introduction of low-dose oxygen. According to the Landau-Lifshitz equation [11], the ferromagnetic resonance frequency (f_r) is proportional to $(H_k \times 4\pi M_s)^{1/2}$,

and the static permeability (μ_s) is expressed as $\mu_s = 1+4\pi M_s/H_k$ for thin films with IPUMA [12-16]. Therefore, we can expect to achieve a significant improvement in the response of real permeability to frequency. The real (μ') and imaginary (μ'') permeability spectra of the oxygen-doping films are shown in Fig. 4. The real permeability of the $Fe_{62}Co_{32}Cr_6$–O alloy film deposited at $R(O_2)$ = 0.6% is as high as ~800 at a frequency up to 1.8 GHz and maintains 200 at ~2.8 GHz. When $R(O_2)$ increases to 1.3%, the real permeability declines compared to the case of $R(O_2)$ = 0.6%, but it can still maintain a value of 200 at frequencies up to ~3.3 GHz.

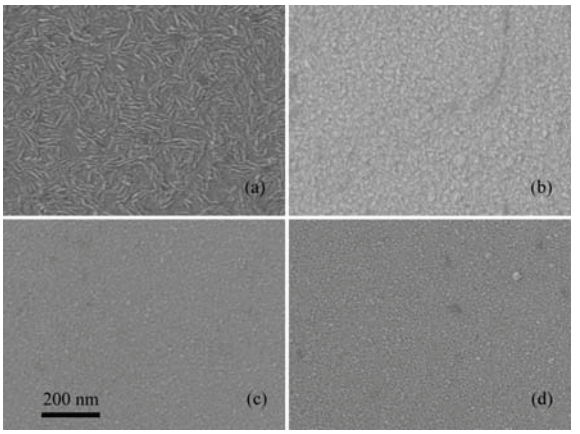

Fig. 2. SEM images of the $Fe_{62}Co_{32}Cr_6$–O thin films deposited at R (O2) = (a) 0%, (b) 0.6%, (c) 1.3%, and (d) 6.3%.

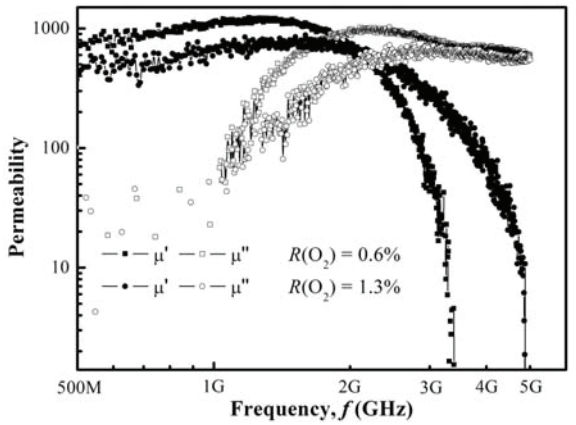

Fig. 4. Permeability spectra (μ ~ f) for the $Fe_{62}Co_{32}Cr_6$–O thin films deposited at R (O2) = 0.6% and 1.3%.

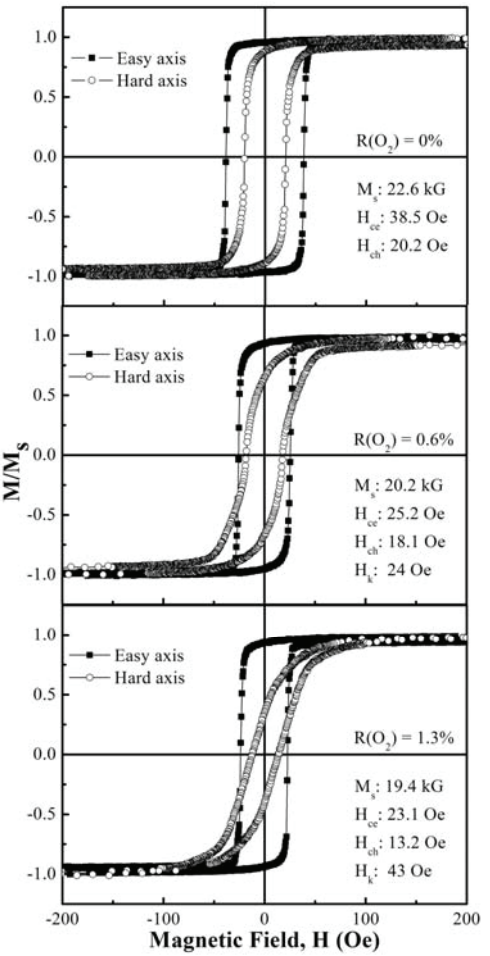

Fig. 3. Hysteresis loops for the $Fe_{62}Co_{32}Cr_6$–O thin films deposited at different $R(O_2)$.

4. Summary

We prepared a series of $Fe_{62}Co_{32}Cr_6$–O films using double-target magnetron co-sputtering by changing the oxygen gas flow ratio. The high-frequency magnetic performance of $Fe_{62}Co_{32}Cr_6$–O films can be well controlled by adjusting the amount of oxygen introduced into the films. At an optimized condition of

$R(O_2)$ = 1.3%, a high saturation magnetization of 19.4 kG, and a suitable IPUMA field of 43 Oe were achieved. Under this optimized condition, the obtained films have a high real permeability of ~200 at frequency up to 3.3 GHz. The combination of high saturation magnetization, adjustable and larger IPUMA field, and high resistivity in the GHz range makes the $Fe_{62}Co_{32}Cr_6$–O films become a promising candidate as future magnetic materials for high-frequency electromagnetic devices in the gigahertz range.

Acknowledgements

This work was supported by the National Basic Research Program of China (No. 2012CB933103) and the National Natural Science Foundation of China (Grant No. 50971108, 50825101, and 51171158).

References

[1] Jin S, Zhu W, van Dover RB, Tiefel TH, Korenivski V, Chen LH. *Appl Phys Lett* 1997;**70**:3161-3163.
[2] Li ZW, Chen LF, Wu YP, Ong CK. *J Appl Phys* 2004;**96**:534-539.
[3] Ohnuma S, Kobayashi N, Masumoto T, Mitani S, Fujimori H. *J Appl Phys* 1999;**85**:4574-4576.
[4] Wang GW, Zhang F, Zuo HP, Yu ZH, Ge SH. *Nanoscale Res Lett* 2010;**5**:1107-1110.
[5] Ohnuma S, Lee HJ, Kobayashi N, Fujimori H, Masumoto T. *IEEE Trans Magn* 2001;**37**:2251-2254.
[6] Ge SH, Yao DS, Yamaguchi M, Yang XL, Zuo HP, Ishii T, Zhou D, Li FS. *J Phys D: Appl Phys* 2007;**40**:3660-3664.
[7] Hayakawa Y, Makino A, Fujimori H, Inoue A. *J Appl Phys* 1997;**81**:3747-3752.
[8] Vas'ko VA, Inturi VR, Riemer SC, Morrone A, Schouweiler D, Knox RD, Kief MT. *J Appl Phys* 2002;**91**:6818-6820.
[9] Wang W, Chen Y, Yue GH, Sumiyama K, Hihara T, Peng DL. *J Appl Phys* 2009;**106**:013912.
[10] Zuo HP, Ge SH, Wang ZK, Xiao YH, Yao DS. *Scripta Mater* 2010;**62**:766-769.
[11] Gilbert TL. *IEEE Trans Magn* 2004;**40**:3443-3449.
[12] Chai GZ, Yang YC, Zhu JY, Lin M, Sui WB, Guo DW, Li XL, Xue DS. *Appl Phys Lett* 2010;**96**:012505.
[13] Snoek JL. *Nature* 1947;**160**:90-90.
[14] Snoek JL. *Physica* 1948;**14**:207-217.
[15] Queste S, Dubourg S, Acher O, Barholz KU, Mattheis R. *J Appl Phys* 2004;**95**:6873-6875.
[16] Acher O, Adenot AL. *Phys Rev B* 2000;**62**:11324-11327.